# Single scattering by red blood cells

Martin Hammer, Dietrich Schweitzer, Bernhard Michel, Eike Thamm, and Achim Kolb

A highly diluted suspension of red blood cells (hematocrit 0.01) was illuminated with an Ar or a dye laser in the wavelength range of 458–660 nm. The extinction and the angle-resolved intensity of scattered light were measured and compared with the predictions of Mie theory, the Rayleigh–Gans approximation, and the anomalous diffraction approximation. Furthermore, empirical phase functions were fitted to the measurements. The measurements were in satisfactory agreement with the predictions of Mie theory. However, better agreement was found with the anomalous diffraction model. In the Rayleigh–Gans approximation, only small-angle scattering is described appropriately. The scattering phase function of erythrocytes may be represented by the Gegenbauer kernel phase function. © 1998 Optical Society of America

*OCIS codes:* 170.0170, 170.1470, 170.1530, 170.7050, 290.0290, 290.5820.

## 1. Introduction

The medical application of light for diagnostic purposes as well as for surgical use of lasers requires a description of the distribution of radiant energy in irradiated tissue. This description can be given by a rigorous[1] or approximate[2] solution of the radiative transfer equation or by a Monte Carlo simulation.[2] However, there is a need for information on the scattering and the absorbing behavior of the tissue for all these methods. This information can be given in terms of scattering coefficient $\mu_s$ and absorption coefficient $\mu_a$, which are inversely proportional to the respective mean free path lengths, and by the scattering phase function. The absorption coefficient is related to absorption cross section $\sigma_a$ of a single-scattering and absorbing particle by $\mu_a = (H/V)\sigma_a$, where $H$ is the volume fraction of scatterers in the medium and $V$ is the volume of the scatterer. For densely packed tenuous scatterers, Twersky[3] derived the approximate relation

$$\mu_s = \frac{H(1-H)}{V}\,\sigma_s$$

between $\mu_s$ and the scattering cross section $\sigma_s$.

Because biological structures are complex, it is generally difficult to study single scatterers. However, there is an important exception, the red blood cell. First, the erythrocyte is important for tissue optics because it contains one of the strongest absorbers of visual light in the human body, hemoglobin. Second, erythrocytes can easily be isolated and studied experimentally. Third, the erythrocyte does not show an internal structure, providing the opportunity to apply theoretical models of scattering to these cells.

For all these reasons, red blood cells have been widely studied in previous investigations. Reynolds *et al.*[4] assumed that the erythrocyte obeys Mie scattering. The absorption and the scattering cross sections obtained from Mie theory were also used by Schmitt *et al.*[5] and Steinke and Shepherd,[6] who described light transport in whole blood by applying the diffusion approximation. Tycko *et al.*[7] found good agreement in flow cytometric measurements of erythrocytes after isovolumetrically sphering with Mie theory. Despite the deviation of the form of the native red blood cell from the sphere, Steinke and Shepherd[8] showed that their scattering experiment corresponds well with Mie theory at 633 nm. However, they did not compare their data with other scattering theories, and they did not consider shorter wavelengths at which the absorption by hemoglobin is much stronger. Borovoi and Naats[9] calculated the small-angle scattering amplitude of the erythrocyte by using the anomalous diffraction theory, but they did not compare their results with measurements. Since the refractive index of the hemoglobin solution inside the cells is close to that in blood

plasma, the Rayleigh–Gans scattering theory should also be applicable.

The goal of this research is to compare the theories mentioned above, which are briefly explained in Section 2, with the data from scattering experiments performed over nearly the whole visible wavelength range. The optical properties of the erythrocytes used in the calculations are given in Section 3. The experiment is described in Section 4, and the results are in Section 5. In addition to the appropriate theoretical description of the observed scattering behavior of the cells, a practically applicable scattering phase function was sought. Furthermore, the results are compared with those obtained from double integrating sphere measurements by Roggan et al.[10] and Yaroslavsky et al.[11,12]

## 2. Theory

We assume a plane electromagnetic wave with an amplitude of unity propagating in the positive $z$ direction, which is incident on a particle. At a sufficient distance the electromagnetic field $\mathbf{E}$ scattered by this particle may be described by[13]

$$\mathbf{E}(\mathbf{r}) = \mathbf{f}(\hat{\mathbf{r}}) \frac{\exp(ikR)}{R} \qquad (1)$$

with the scattering amplitude $\mathbf{f}(\hat{\mathbf{r}})$ given by

$$\mathbf{f}(\hat{\mathbf{r}}) = \frac{k^2}{4\pi} \int_{V'} \mathbf{E}(\mathbf{r'})[\varepsilon_r(\mathbf{r'}) - 1]\exp(-ik\hat{\mathbf{r}} \cdot \mathbf{r'})\mathrm{d}^3\mathbf{r'}. \qquad (2)$$

Here $\hat{\mathbf{r}}$ is the unit vector in the direction of the scattered wave, $\mathbf{k}$ is the wave number, $R$ is the distance from the scatterer, $\varepsilon_r$ is the relative dielectric constant of the scatterer, and the integration has to be performed over all points $\mathbf{r'}$ within its volume $V$. A scattering particle may be characterized by its scattering cross section

$$\sigma_s = \int_{4\pi} |\mathbf{f}(\hat{\mathbf{r}})|^2 \mathrm{d}\omega, \qquad (3)$$

which is an integral over all scattering angles, the extinction cross section

$$\sigma_{\mathrm{ext}} = \frac{4\pi}{k} \, \mathrm{Im}[\hat{\mathbf{e}}_p \cdot \mathbf{f}(\hat{\mathbf{e}}_z)], \qquad (4)$$

where $\hat{\mathbf{e}}_p$ and $\hat{\mathbf{e}}_z$ are unit vectors of the polarization and in the $z$ direction, respectively, and by the scattering phase function

$$p(\hat{\mathbf{r}}) = \frac{4\pi}{\sigma_{\mathrm{ext}}} |\mathbf{f}(\hat{\mathbf{r}})|^2, \qquad (5)$$

which is normalized to the albedo $W_0$ of the particle:

$$W_0 = \frac{\sigma_s}{\sigma_{\mathrm{ext}}} = \frac{1}{4\pi} \int_{4\pi} p(\hat{\mathbf{r}})\mathrm{d}\omega. \qquad (6)$$

Cross sections $\sigma_s$ and $\sigma_{\mathrm{ext}}$ depend on the polarization of the incident radiation. In our experiments we measured the scattering close to the forward direction only. In this case Mie theory predicts only a weak change in the polarization, and the Rayleigh–Gans as well as the anomalous diffraction approximation does not predict a change in the polarization state at all. Since polarization is unimportant for our considerations, the unit vector of polarization is omitted throughout this paper.

The absorption cross section may be obtained from the integration of the imaginary part of the dielectric constant and the electric field over the volume of the scatterer:

$$\sigma_a = \int_V k \cdot \varepsilon_r'' |E(\mathbf{r'})|^2 \mathrm{d}^3\mathbf{r'}. \qquad (7)$$

### A. Mie Scattering

The scattering problem may be analytically solved for a homogeneous spherical particle resulting in[14]

$$\sigma_s = \frac{2\pi}{k^2} \sum_{n=1}^{\infty} (2n + 1)(|a_n|^2 + |b_n|^2),$$

$$\sigma_{\mathrm{ext}} = \frac{2\pi}{k^2} \sum_{n=1}^{\infty} (2n + 1)\mathrm{Re}\{a_n + b_n\}, \qquad (8)$$

and the phase function

$$p(\vartheta) = \frac{1}{k^2 r^2} (|S_1|^2 + |S_2|^2), \qquad (9)$$

where $\vartheta$ is the scattering angle between $\hat{\mathbf{e}}_z$ and $\hat{\mathbf{r}}$ and

$$S_1(\vartheta) = \sum_{n=1}^{\infty} \frac{2n + 1}{n(n + 1)}$$
$$\times \left[ a_n \frac{P_n^{1}(\cos \vartheta)}{\sin \vartheta} + b_n \frac{d}{d\vartheta} P_n^{1}(\cos \vartheta) \right],$$

$$S_2(\vartheta) = \sum_{n=1}^{\infty} \frac{2n + 1}{n(n + 1)}$$
$$\times \left[ b_n \frac{P_n^{1}(\cos \vartheta)}{\sin \vartheta} + a_n \frac{d}{d\vartheta} P_n^{1}(\cos \vartheta) \right]. \qquad (10)$$

Here $P_n^{1}(\cos \vartheta)$ are the associated Legendre functions and $a_n$ and $b_n$ depend on the Riccati–Bessel functions of the size parameter and the relative refractive index $n_r = \sqrt{\varepsilon_r}$. The absorption cross section is given by $\sigma_a = \sigma_{\mathrm{ext}} - \sigma_s$.

Computer programs by Bohren and Huffman[14] were used in all the Mie calculations.

### B. Rayleigh–Gans Scattering

If $D$ is the typical cross-sectional extent of the particle and $(\varepsilon_r - 1)kD \ll 1$, the electric field $E(\mathbf{r})$ inside the particle can be approximated by the incident field

$E_i = \exp(ik\mathbf{r} \cdot \hat{\mathbf{e}}_z)$. Using this approximation in Eq. (2) and introducing $\mathbf{k}_s = k(\hat{\mathbf{e}}_z - \hat{\mathbf{r}})$, we find that

$$f(\mathbf{k}_s) = \frac{k^2}{4\pi} \int_{V'} (\varepsilon_r - 1)\exp(i\mathbf{k}_s \cdot \mathbf{r})\mathrm{d}^3 r', \qquad (11)$$

which is the Rayleigh–Gans approximation for the scattering amplitude. For red blood cells and light with a wavelength of 577 nm, we have $D \approx 5.5$ μm, $k = 10.9$ μm$^{-1}$, and $\varepsilon_r \approx 1.11$, and therefore $(\varepsilon_r - 1)kD \approx 6.6$, which exceeds the range of validity of the Rayleigh–Gans approximation. Nevertheless we expect this approximation to reproduce correctly at least the qualitative features of the scattering by erythrocytes. Quantitative results should, however, be benchmarked against the predictions of other methods.

When one is investigating diluted blood, it is reasonable to assume that the cells are randomly oriented in space. When one is performing an orientational average of Eq. (11), it is convenient to introduce the index function[15]

$$\eta(\mathbf{r}, \tau) = \begin{cases} 1 \text{ inside the particle} \\ 0 \text{ elsewhere} \end{cases}, \qquad (12)$$

where the identifier $\tau$ specifies the spatial orientation of the particle. We assume the particle to be axially symmetric about an arbitrary axis, with $\hat{\mathbf{a}}$ being the unit vector pointing in the direction of this axis. The index function can then be written in the form

$$\eta(\mathbf{r}, \hat{\mathbf{a}}) = H[\xi(\cos v) - r], \qquad \cos v = \hat{\mathbf{r}} \cdot \hat{\mathbf{a}}, \quad (13)$$

where $\xi(\cos v) - r$ is a parameterization of the particle's surface and $H(x)$ is the Heaviside step function $H(x) = 0$ for $x \leq 0$ and $H(x) = 1$ for $x > 0$. The orientational average of the index function $\chi(r) = \langle \eta(\mathbf{r}, \hat{\mathbf{a}}) \rangle_{\hat{a}}$ is spherically symmetric and given by

$$\chi(r) = \frac{1}{2} \int_{-1}^{1} H[\xi(x) - r]\mathrm{d}x. \qquad (14)$$

On orientational averaging of the scattering amplitude, we obtain

$$\langle f(\mathbf{k}_s) \rangle = k(\varepsilon_r - 1) \int_0^{\infty} r\chi(r)\sin(k_s r)\mathrm{d}r. \qquad (15)$$

Erythrocytes are discoid particles. Their surface can be parameterized by

$$\xi(\cos v) = 3(\sin v)^4 + 0.75, \qquad (16)$$

where 1 μm is used as the length unit. Substituting Eq. (16) into Eq. (14), we get

$$\chi(r) = \begin{cases} 1 & \text{for } 0 \leq r \leq 0.75, \\ \left[ 4 - 2\left(\frac{4}{3}r - 1\right)^{1/2} \right]^{1/2} & \text{for } 0.75 < r \leq 3.75. \\ 0 & \text{for } r > 3.75 \end{cases}$$
$$(17)$$

With this result the scattering amplitude can be calculated by a straightforward numerical integration of Eq. (15). The absorption cross section follows from Eq. (7):

$$\sigma_a = k \cdot \varepsilon_r'' \cdot V. \qquad (18)$$

## C. Anomalous Diffraction Theory

On the condition that the relative refractive index $n_r = \sqrt{\varepsilon_r}$ is close to unity ($n_r - 1 \ll 1$) and the characteristic dimension of the scatterer is large compared with the wavelength, anomalous diffraction theory is applicable. Red blood cells are too small for the unrestricted application of this theory, in contrast to the Rayleigh–Gans approximation, for which the blood cells are too large. In the anomalous diffraction theory it is assumed that the refraction of the incident plane wave does not alter the direction of propagation. However, the wave suffers a phase lag. For a plane wave propagating in the $z$ direction the phase lag is a function of the $x$ and the $y$ coordinates and is given as

$$\Phi(x, y) = k \int [n_r\eta(x, y, z) - 1]\mathrm{d}z, \qquad (19)$$

where $\eta(x, y, z)$ is the index function of the particle introduced in Subsection 2.B. The integration in Eq. (19) is preformed over the thickness of the particle in the $z$ direction. Thus the particle is represented by a phase plate according to Eq. (19), and the scattering amplitude in the far field can be obtained from the Fraunhofer diffraction integral,[9]

$$f(\vartheta, \varphi) = \frac{k}{2\pi i} \int \exp[-ik \sin \vartheta(x \cos \varphi + y \sin \varphi)]$$
$$\times \{\exp[i\Phi(x, y)] - 1\}\mathrm{d}x\mathrm{d}y, \qquad (20)$$

over the shadow of the particle.

## D. Empirical Phase Functions

All phase functions derived from rigorous or approximate solutions of the scattering problem in the subsections above are functions either of infinite series or of integrals that in general cannot be solved analytically. Thus convergent series approximations to the phase function are often used to solve the radiation transport problem. Assuming an azimuthal symmetry of the scattering event, the phase function has to fulfill the normalization condition

$$\int_{-1}^{1} p(\mu)\mathrm{d}\mu = W_0 \text{ with } \mu = \cos \vartheta. \qquad (21)$$

The most popular one is the Henyey–Greenstein phase function[16] that is an infinite series of Legendre polynomials converging to

$$p(\mu) = \frac{1}{4\pi W_0} \frac{1 - g^2}{(1 + g^2 - 2g\mu)^{3/2}}, \qquad (22)$$

where $g$ describes the anisotropy of scattering and may vary between $-1$ and $1$. A generalization has been proposed by Reynolds and McCormick[17] using a series of Gegenbauer polynomials converging to

$$p(\mu) = \frac{\alpha g}{\pi W_0}$$

$$\times \frac{(1 - g^2)^{2\alpha}}{[(1 + g)^{2\alpha} - (1 - g^{2\alpha})](1 + g^2 - 2g\mu)^{(1+\alpha)}}$$

$$\text{with } |g| \le 1, \alpha > -\frac{1}{2}. \quad (23)$$

This Gegenbauer kernel phase function results in the Henyey–Greenstein phase function for $\alpha = 1/2$. We fitted both phase functions to the goniophotometric measurements of light scattered by erythrocytes by using the Maquard–Levenberg algorithm. Besides the parameters $g$ and $\alpha$ the mean cosine of the scattering angle

$$\bar{\mu} = \frac{\int_{-1}^{1} \mu p(\mu) \mathrm{d}\mu}{W_0} \quad (24)$$

was determined.

### 3. Optical Properties of the Erythrocyte

All the scattering theories described in Section 2 require information on the size and the shape of the scattering particle as well as on the real and the imaginary part of its refractive index, which is given below. The normal human red blood cell has a biconcave discoid shape that may be represented by Eq. (14), resulting in a disk diameter of 6.75 $\mu$m. The cell consists of a lipid bilayer membrane with a thickness[18] of 7 nm and a refractive index[19] of $\sim 1.46$ filled with aqueous hemoglobin solution. Since the membrane is very thin and its refractive index is not so far from that of the blood plasma outside and the cytoplasm inside the cell, its influence on scattering was neglected. The mean hemoglobin concentration is taken as[20] $c = 340$ g/l. The imaginary part $n''$ of the refractive index $n$ is related to the molar absorption coefficient $\varepsilon_\mu$ by[21]

$$n'' = \ln(10) \frac{\lambda}{4\pi} \varepsilon_\mu(\lambda)c, \quad (25)$$

where $\lambda$ is the wavelength. The absorption spectra of hemoglobin were obtained from van Assendelft.[22]

The real part of the refractive index has been given by Tycko $et$ $al.$[7] as $n' = 1.40$. However, owing to the hemoglobin absorption bands in the blue and green spectral range, dispersion must be taken into account. We did this using approximate formulas for liquids given by Latimer.[23] The calculated values for the real and the imaginary part of the refractive index are given in Fig. 1.
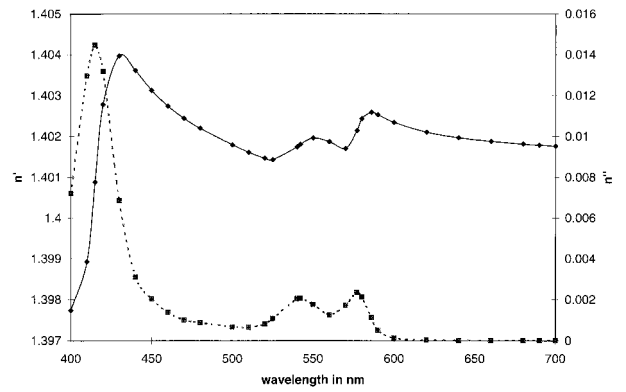


Fig. 1. Refractive index of erythrocytes: solid curve, real part $n'$; dashed–dotted curve, imaginary part $n''$.

### 4. Experimental Setup and Procedures

Human whole blood was obtained from healthy donors. The erythrocytes were separated from the blood plasma and the white cell fraction by centrifugation at 3200 rpm for 10 min and were washed three times in an isotonic phosphate buffer ($pH = 7.4$, $n = 1.33$). The red blood cell suspension was diluted in isotonic phosphate buffer to a hematocrit of 0.01. The hematocrit, the hemoglobin concentration, and the number and volume of erythrocytes of each sample were determined with a Cell-Dyn 1700 (Abbott, Germany). All scattering experiments were performed with fully oxygenated erythrocytes. For insuring full oxygenation, the specimens were bubbled with pure oxygen immediately before the measurement.

The measurements were carried out on a homemade goniophotometer. An argon-ion laser, ILA190 (Carl Zeiss Jena, Germany), was used as a light source for wavelengths of 458–514 nm, and an argon-pumped tunable dye laser (Zentrum für wissenschaffLichen Geräteban, Germany) was used for wavelengths of 543–660 nm. Both lasers ran in the cw mode. Dependent on the wavelength, the typical power at the specimen was 3–15 mW and the spot diameter was 2 mm. The beam divergence of the argon laser was 0.5 mrad, and that of the dye laser was 1.5 mrad. The wavelength was adjusted to an accuracy of 0.2 nm and controlled with a wavelength sensor, Wave Check (Angewandte Physik & Electronik GmbH, Germany). The laser beam was directed onto a quartz cuvette (Helma Optik, Germany) containing the diluted blood sample. The thickness of the cuvette was 100 $\mu$m for the transmission measurement. In the measurement of the phase function we used a cuvette with a thickness of 10 $\mu$m containing a single-cell layer. No erythrocyte aggregation occurred, which was checked by microscopic inspection. An attempt to examine flowing blood was not successful since the hematocrit of the extremely diluted blood sample was not sufficiently stable within the laser spot in flow conditions.

The scattered light and a reference beam were measured by a laser power meter, Rm 6600 (Laser

Probe, N.Y.), equipped with two probes: RkP-575 (1 mW–10 W) and RkP-576 (1 nW–1 mW). The latter was positioned behind a pinhole with a diameter of 1.3 mm at a distance of 55 cm from the cuvette containing the blood sample, resulting in an aperture solid angle of $4.4 \times 10^{-6}$ sr. The detector was rotated around the cuvette with a positioning precision of 0.1 deg. Measurements of the phase function were taken in the range from 0.75 to 15 deg. These values were corrected for the refraction due to the different refractive indices of water and air. The measurement of either a complete wavelength scan or a complete angular scan took less than 10 min. No sedimentation of the cells in the cuvette was observed during this time. For avoiding the influence of ambient light, the illumination was chopped and a lock-in technique was used.

The scattering phase function was directly measured as the angular distribution of the scattered light intensity. In the forward direction the transmission

$$T = \exp[-(\mu_a + \mu_s)d]$$
$$= \exp\left\{-\left[\frac{H}{V}\sigma_a + \frac{H(1-H)}{V}\sigma_s\right]d\right\} \quad (26)$$

of a sample with thickness $d$ was measured as the ratio of the light transmitted through the cuvette filled with the sample to one filled with water. The extinction cross section was calculated as

$$\sigma_{\text{ext}} = \sigma_a + \sigma_s = \frac{V}{Hd}\ln T, \quad (27)$$

neglecting the factor $(1 - H)$, which was ~0.99. The experimental conditions were unchanged with the exception of the thickness of the cuvette.

An important condition for the measurement of the scattering phase function and the cross section is that the distance between the single scatterers is so large that interference from the waves scattered at two neighboring particles is negligible. To check this for the used volume fraction of scatterers ($H = 0.01$), we performed a measurement on latex spheres. As shown in Fig. 2, the measured phase function is in good agreement with the predictions of Mie theory. This also holds for the scattering cross section. Thus the described optical arrangement seems to be capable of measuring the single-scattering cross section and phase function of a suspension containing 1% scatterers.

## 5. Results

### A. Angle-Resolved Measurements

Measurements of the intensity of scattered light were taken at the following wavelengths: 458, 496, 514, 543, 548, 555, 560, 565, 569, 572.5, 577, 580, 586, 592, 600, 610, 630, and 660 nm for 20 scattering angles between 0.75 and 14.9 deg. For each wavelength and each angle, ten measurements were performed and averaged. Typically, intensity decreased by
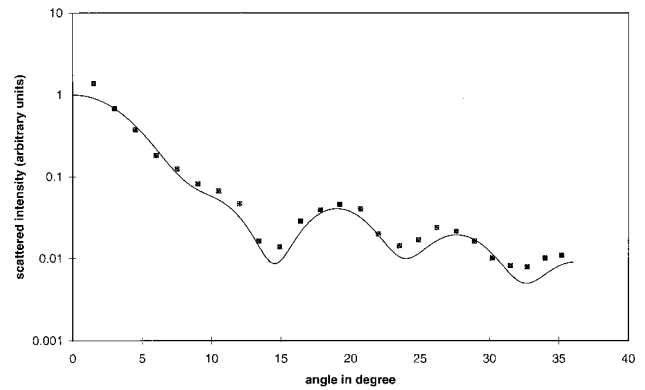


Fig. 2. Scattering phase function of latex speres in water: solid curve, Mie calculation; squares, measurement.

~2.5 log units in this angular range. A dependence of the phase function on the wavelength, and therefore on hemoglobin absorption, was not observed. As a typical example the angular intensity distribution is shown in Fig. 3 for the hemoglobin absorption peak at 577 nm. The bars indicate the standard deviation of ten measurements on the same sample.

### 1. Scattering Models

The measured phase functions were compared with the predictions of the theoretical scattering models described in Section 2. As can be seen in Fig. 3, good agreement with the Rayleigh–Gans theory is given only within an angular region as large as ~4 deg. However, at larger angles the scattering amplitude is clearly underestimated by this approximation.

Quite a good representation of the phase function is given by Mie theory over the entire measured angular range. However, the typical lobe pattern, as seen in the microsphere experiment (Fig. 2), was not observed. Instead the lobe pattern of the phase function was averaged out by including the distribution of the cell volume (Fig. 7).

The phase function according to the anomalous diffraction theory was calculated for ten different orien-
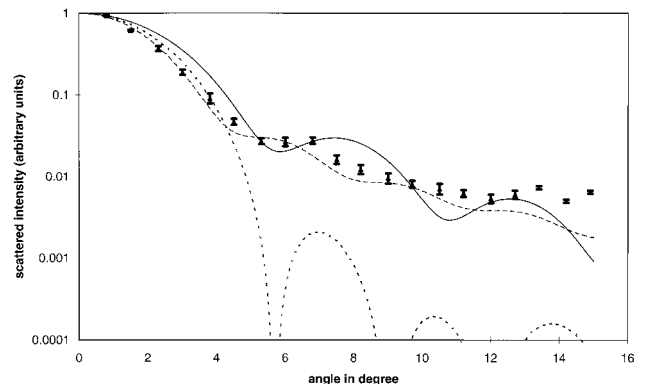


Fig. 3. Scattering phase function of red blood cells at 577 nm: symbols, measurement; solid curve, Mie theory; dashed curve, anomalous diffraction; dotted curve, Rayleigh–Gans approximation.

| Parameters | Mie Theory | Rayleigh–Gans Scattering | Anomalous Diffraction |
|---|---|---|---|
| Mean value | 0.118 | 0.060 | 0.041 |
| Standard deviation | 0.111 | 0.066 | 0.039 |

tations of the cell in the illuminating beam. The cell was rotated around an axis perpendicular to the beam from 0 to 90 deg, and the scattering amplitudes were determined parallel and perpendicular to that axis and averaged over all orientations. Figure 3 shows quite good agreement with the measurement.

To compare the agreement of the different theoretically determined phase functions with the angle-resolved measurements, we calculated the sum of the quadratic deviations between the scattering model calculations and the experiment over all angles for all wavelengths. The averages over the wavelengths as well as the standard deviations are given in Table 1.

## 2. Empirical Phase Functions

Roggan *et al.*[10] found the small-angle scattering for erythrocytes ($\theta < 2$ deg), as predicted by the Henyey–Greenstein phase function, to be too large when compared with the Mie-scattering phase function. They used the two-parameter Gegenbauer kernel phase function proposed by Reynolds and McCormick[17] that has been successfully fitted to goniophotometric measurements at 633 nm by Yaroslavsky *et al.*[11] Thus we fitted our goniophotometric measurements with the Henyey–Greenstein phase function as well as with the Gegenbauer kernel phase function. A typical example is shown in Fig. 4. (Note the logarithmic scaling of the scattering intensity.) Since the Gegenbauer phase function is a generalization of the Henyey–Greenstein phase function with two independent parameters, the fit is necessarily better for the Gegenbauer phase function (mean square error, 0.055 versus 0.18 for the Henyey–Greenstein phase function in the given example at 577 nm). However, analyzing all fits of the Gegenbauer kernel phase function, we found a strong quadratic dependence (correlation coefficient, 0.976) between parameters $\alpha$ and $g$ in Eq. (23).

Therefore the degree of freedom was reduced by fixing $\alpha$. For finding the appropriate $\alpha$ value, one-parameter fits with fixed $\alpha$ were performed for all measured phase functions. Figure 5 shows the sum of the mean-square errors of all fits for $\alpha$ between 0.5 (Henyey–Greenstein phase function) and 3. A minimum of mean-square errors was found at $\alpha = 1.5$.

## 3. Anisotropy of Scattering

With respect to the solution of the radiation transport problem in scattering media (e.g., in the diffusion approximation), the anisotropy of the single-scattering event is an important quantity. The anisotropy may be given by the mean cosine of scattering angle $\bar{\mu}$, which was calculated by Mie the-
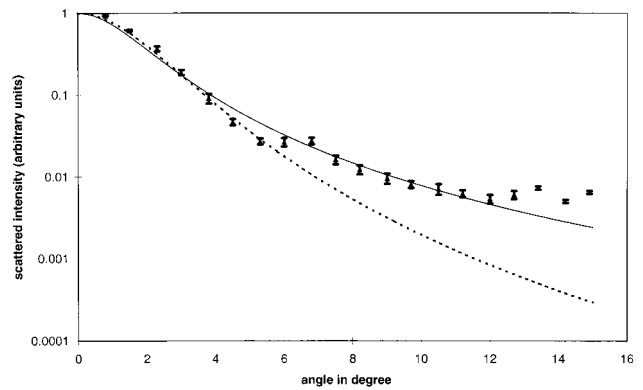


Fig. 4. Scattering phase function of red blood cells at 577 nm: symbols. measurement; solid curve, Henyey–Greenstein phase function; dotted curve, Gegenbauer kernel phase function ($\alpha = 1.5$).

ory to be $0.9914 \pm 0.00065$ for an erythrocyte with a volume of 90 $\mu m^3$ over the considered wavelength range. The Rayleigh–Gans model results in an unrealistically high value of $0.9995 \pm 0.00008$ because of the steep decrease of its scattering amplitude toward larger angles. In contrast, the fit of the Henyey–Greenstein phase function yields too small a value for $\bar{\mu}$, namely, $0.9655 \pm 0.0043$, indicating that this is not an optimal phase function for scattering by erythrocytes. The value of $\bar{\mu}$ obtained from the Gegenbauer kernel phase function ($\alpha = 1.5$) is $\bar{\mu} = 0.9973 \pm 0.00059$, in good agreement with the value from Mie theory. It must be emphasized that these values are valid for erythrocytes suspended in aqueous buffer solution with a refractive index of 1.33. Since the refractive index of blood plasma is higher, the anisotropy must be higher in whole blood, as shown by Steinke and Shepherd.[8] The anomalous diffraction theory is valid only for small-angle scattering, and its ray-tracing program does not give the scattering amplitude for the entire angle range. Therefore the mean cosine of the scattering angle defined in Eq. (24) cannot be calculated for this scattering model.
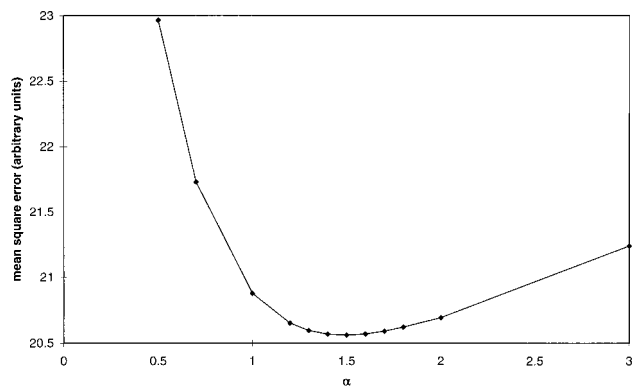


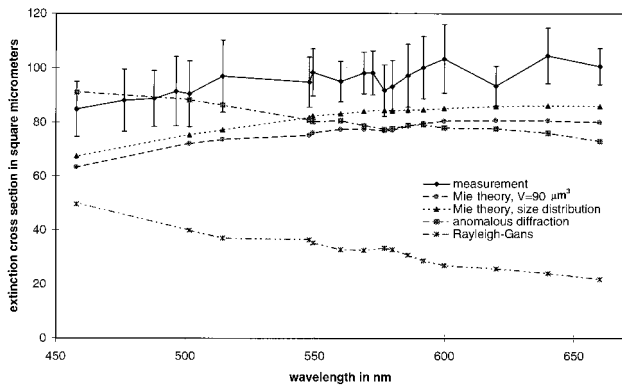Fig. 5. Mean-square deviation of the fitted Gegenbauer kernel phase function from the measurements versus parameter $\alpha$.

Fig. 6.   Extinction cross section of erythrocytes.



Fig. 7.   Volume distribution of the erythrocytes in the examined specimen.

## B.   Extinction Measurements

Transmission was measured and averaged 20 times per wavelength.   The extinction cross section was calculated according to Eq. (27).   The results are shown in Fig. 6.   The error bars indicate the standard deviation of subsequent measurements on ten samples taken from the same specimen.   Since the error of a single measurement is much smaller, this rather large standard deviation is expected to result from inevitable differences in the hematocrit of the samples.   Thus we can estimate the extinction cross section of a single red blood cell to be ~95 $\mu m^2$.   As a general trend, $\sigma_{ext}$ increases slightly as the wavelength increases.

These experimental results were compared with the cross sections obtained from the scattering models (see Section 2).   The Mie calculation was performed first for a fixed volume of the scatterer (90 $\mu m^3$).   Furthermore, the Mie calculation was repeated for an ensemble of scatterers showing the same volume distribution as was found in the specimen (Fig. 7).   This results in extinction cross sections that are somewhat closer to the measured values.   However, in general the extinction cross section is underestimated by ~15% by Mie theory.   The anomalous diffraction theory gives extinction cross sections that fall slightly as wavelength increases.   The values are comparable with that of Mie theory.   However, the Rayleigh–Gans approximation yields extinction cross sections much smaller than the measured ones.   This is a result of the highly anisotropic scattering (see Fig. 3), which, according to Eq. (3), results in scattering cross-section values that are too low.   For clarifying and summarizing the differences between the three models, the predicted absorption and scattering cross sections are shown in Fig. 8 and given in Table 2.

## 6.   Discussion

Mie theory has been applied widely to describe light scattering by red blood cells.[4,7,8,12]   Steinke and Shepherd[8] performed scattering experiments showing good agreement between measured scattering cross sections and those calculated.   They measured a scattering cross section of 81.24 $\mu m^2$, which is sim-
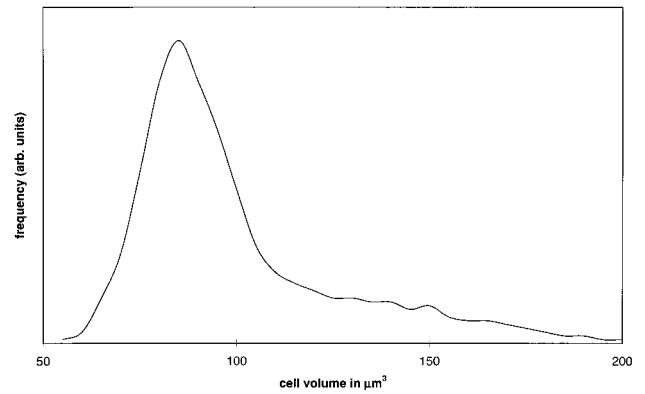
ilar to the value that we found.   Comparing goniophotometric measurements on a 0.1-mm-thick layer of whole blood with Monte Carlo simulations by using different phase functions, Yaroslavky et al.[12] also found that the Mie phase function agreed better with experiment than the Henyey–Greenstein or Gegenbauer kernel phase function.   Our measurements confirmed the applicability of Mie theory to the scattering by erythrocytes despite the deviation of the cell from the spherical form.   However, for scattering angles of less than 5 deg, the scattered intensity is overestimated by this scattering model.   The best agreement of the experimentally obtained phase function with theory, for scattering angles between 0.75 and 15 deg, was obtained with the anomalous diffraction theory.   The Rayleigh–Gans approximation gives quite good results for small-angle scattering but does not adequately describe the scattering over the entire angle range.   This results in the obvious underestimation of the scattering coefficient by the Rayleigh–Gans model.   Although the scattering of light by red blood cells into the investigated range of scattering angles is best described by the anomalous diffraction theory, followed by the Rayleigh–Gans approximation, and then Mie-scattering theory (see Table 1), the differences in the mean-square de-
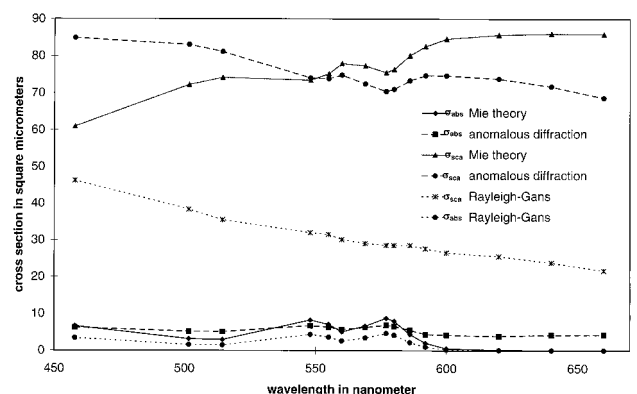


Fig. 8.   Theoretical calculations of scattering and absorption cross sections of erythrocytes.

**Table 2. Scattering and Absorption Cross Sections Calculated from Mie, Rayleigh–Gans, and Anomalous Diffraction Theories**

| Wavelength (nm) | $\sigma_{abs}$ Mie Theory | $\sigma_{abs}$ Anomalous Diffraction | $\sigma_{abs}$ Rayleigh–Gans | $\sigma_{sca}$ Mie Theory | $\sigma_{sca}$ Anomalous Diffraction | $\sigma_{sca}$ Rayleigh–Gans |
|---|---|---|---|---|---|---|
| 458.00 | 6.61 | 6.20 | 3.39 | 60.92 | 84.86 | 46.21 |
| 501.70 | 3.09 | 5.14 | 1.52 | 72.24 | 83.03 | 38.33 |
| 514.50 | 2.92 | 5.08 | 1.43 | 74.18 | 81.14 | 35.50 |
| 548.00 | 8.25 | 6.69 | 4.33 | 73.44 | 74.07 | 31.97 |
| 555.00 | 7.03 | 6.30 | 3.63 | 75.21 | 73.89 | 31.53 |
| 560.00 | 5.06 | 5.73 | 2.55 | 77.96 | 74.83 | 30.11 |
| 569.00 | 6.61 | 6.22 | 3.39 | 77.35 | 72.44 | 29.03 |
| 577.00 | 8.77 | 6.84 | 4.63 | 75.53 | 70.41 | 28.58 |
| 580.00 | 7.92 | 6.59 | 4.13 | 76.40 | 71.01 | 28.51 |
| 586.00 | 4.36 | 5.52 | 2.17 | 80.09 | 73.35 | 28.52 |
| 592.00 | 2.02 | 4.36 | 0.98 | 82.58 | 74.73 | 27.63 |
| 600.00 | 0.50 | 4.20 | 0.24 | 84.60 | 74.70 | 26.57 |
| 620.00 | 0.15 | 3.87 | 0.07 | 85.68 | 73.87 | 25.53 |
| 640.00 | 0.07 | 4.23 | 0.03 | 86.02 | 71.76 | 23.84 |
| 660.00 | 0.05 | 4.25 | 0.02 | 85.92 | 68.70 | 21.66 |

viation between measurement and theory are not significant.

Because of the usefulness in the solution of the radiation transport problem, empirical phase functions are often used instead. Yaroslavsky et al.[11] found the Gegenbauer kernel phase function to be a good model for light scattering by erythrocytes. To achieve good agreement between the Gegenbauer kernel phase function and Mie calculations, Roggan et al.[10] assumed the $\alpha$ in Eq. (23) to be unity. In contrast, Yaroslavsky et al.[11] reported a value of 1.82 from a fit to measured data and Reynolds and McCormick[17] found $\alpha = 1.75$ to be in agreement with calculations according to the Rayleigh–Gans theory. Since we found a quadratic dependence of parameters $\alpha$ and $g$, we fixed $\alpha$ at 1.5, the value at which the mean-square error of all fits of the Gegenbauer kernel phase function to the measurements was minimal. This resulted in a mean scattering cosine of 0.997. This value is somewhat higher than the one reported by Steinke and Shepherd,[8] who reported 0.9818 for two free-running parameters.

Yaroslavsky et al.[11,12] and Roggan et al.[10] determined the macroscopic scattering and absorption coefficients by double integrating sphere measurements and subsequent inverse Monte Carlo simulation. Absorption coefficient $\mu_a$ was given by 1.55 mm$^{-1}$ and $\sim$0.8 mm$^{-1}$, respectively, for whole blood with normal hematocrit and osmolarity at a wavelength of 633 nm. When we use $\mu_a = (H/V)\sigma_a$, the above-mentioned values result in an absorption cross section that is roughly comparable with that given by Mie theory. However, the scattering coefficient was strongly dependent on the chosen parameters $\alpha$ and $g$ of the Gegenbauer kernel phase function used in the inverse Monte Carlo simulation. It ranges from 40 to 412 mm$^{-1}$ (Yaroslavsky et al.[11,12]) and was given by $\sim$80 mm$^{-1}$ by Roggan et al.[10] for flowing whole blood in physiological conditions. Unfortunately, the collimated transmission in these experiments was too small for the scattering coefficient and the mean cosine of the scattering an-

gle to be determined independently.[10] Therefore it is impossible to compare their results with ours. On the other hand, Roggan et al.[10] showed good agreement between their results and Mie theory at a hematocrit of 0.075. So it may be argued that the conditions of single scattering are no longer fulfilled in whole blood. Here the distances of the scatterers are of the same order as their typical dimension. Therefore the scatterers cannot be treated as independent. Interference between the single-scattering events has to be taken into account. This interference should be examined in a subsequent investigation.

## References

1. K. Rinzema, B. J. Hoenders, H. A. Ferwerda, and J. J. Ten Bosch, "Analytic calculation of the radiance in an anisotropically scattering medium close to the source," Pure Appl. Opt. **4,** 629–642 (1995).
2. M. S. Patterson, B. C. Wilson, and D. R. Wyman, "The propagation of optical radiation in tissue. I. Models of radiation transport and their application," Laser Med. Sci. **6,** 155–168 (1991).
3. V. Twersky, "Absorption and multiple scattering by biological suspensions," J. Opt. Soc. Am. **60,** 1084–1093 (1970).
4. L. O. Reynolds, C. Johnson, and A. Ishimaru, "Diffuse reflectance from a finite blood medium: applications to the modeling of fiber optic catheters," Appl. Opt. **15,** 2059–2067 (1976).
5. J. M. Schmitt, J. D. Meindl, and F. G. Mihm, "An integrated circuit based optical sensor for *in vivo* measurement of blood oxygenation," IEEE Trans. Biomed. Eng. **33,** 98–107 (1986).
6. J. M. Steinke and A. P. Shepherd, "Diffusion model of the optical absorbance of whole blood," J. Opt. Soc. Am. A **5,** 813–822 (1988).
7. D. H. Tycko, M. H. Metz, E. A. Epstein, and A. Grinbaum, "Flow-cytometric light scattering measurement of red blood cell volume and hemoglobin concentration," Appl. Opt. **24,** 1355–1365 (1985).
8. J. M. Steinke and A. P. Shepherd, "Comparison of Mie theory

and the light scattering of red blood cells," Appl. Opt. **27,** 4027–4033 (1988).

9. A. G. Borovoi and E. I. Naats, "Scattering of light by a red blood cell," J. Biomed. Opt. **3,** 364–372 (1998).

10. A. Roggan, M. Friebe, K. Dörschel, A. Hahn, and G. Müller, "Optical properties of circulating human blood," in *Laser–Tissue Interaction, Tissue Optics, and Laser Welding*, G. P. Delacretaz, L. O. Svaasand, R. W. Steiner, R. Pini, and G. Godlewski, eds., Proc. SPIE **3195,** 51–63 (1998).

11. A. N. Yaroslavsky, I. V. Yaroslavsky, T. Goldbach, and H.-J. Schwarzmaier, "The optical properties of blood in the near infrared spectral range," in *Optical Diagnostics of Living Cells and Biofluids*, D. L. Farkas, R. C. Leif, A. V. Priezzhev, T. Asakura, and B. J. Tromberg, eds., Proc. SPIE **2678,** 314–324 (1996).

12. A. N. Yaroslavsky, I. V. Yaroslavsky, T. Goldbach, and H.-J. Schwarzmaier, "Different phase function approximation to determine optical properties of blood:   a comparison," in *Optical Diagnostics of Biological Fluids and Advanced Techniques in Analytical Cytology*, A. V. Priezzhev, T. Asakura, and R. C. Leif, eds., Proc. SPIE **2982,** 324–330 (1997).

13. A. Ishimaru, *Wave Propagation and Scattering in Random Media* (Academic, New York, 1978).

14. F. G. Bohren and D. R. Huffman, *Absorption and Scattering of Light by Small Particles* (Wiley, New York, 1983).

15. B. Michel, "Statistical method to calculate extinction by small irregularly shaped particles," J. Opt. Soc. Am. A **12,** 2471–2481 (1995).

16. L. G. Henyey and J. L. Greenstein, "Diffuse radiation in the galaxy," Astrophys. J. **93,** 70–83 (1941).

17. L. O. Reynolds and N. J. McCormick, "Approximate two parameter phase function for light scattering," J. Opt. Soc. Am. **70,** 1206–1212 (1980).

18. M. M. Wintrobe, *Clinical Hematology* (Lea and Febiger, Philadelphia, 1981).

19. R. Barer and S. Joseph, "Refractometry of living cells," Q. J. Microsc. Sci. **95,** 399–406 (1954).

20. R. B. Pennell, "Composition of normal human red cells," in *The Red Blood Cell*, C. Bishop and D. M. Surgenor, eds. (Academic, New York, 1964).

21. G. Kortüm, *Reflexionsspektroskopie* (Springer-Verlag, Berlin, 1969).

22. O. W. van Assendelft, *Spectrophotometry of Hemoglobin Derivatives* (Roal Vangorcum, Assen, 1970).

23. P. Latimer, "Anomalous dispersion of $CS_2$ and $CHCL_3$—theoretical predictions," J. Opt. Soc. Am. **51,** 116–118 (1961).